Pasted positive plate of lead–acid battery
General analysis of discharge process

C.V. D'Alkaine[a,*], R.P. Impinnisi[b], J.R. Rocha[b]

[a]*Group of Electrochemistry and Polymers, Chemistry Department, Federal University of São Carlos, São Carlos (SP), Brazil*
[b]*Battery Laboratory, Institute of Technology for Development- LACTEC, Curitiba, (PR)-Brazil*

Abstract

A general analysis of the discharge process of pasted positive plates of lead–acid batteries is presented. Two models are explored in order to understand qualitatively the phenomenon: a solid-state reaction model and a dissolution–precipitation reaction model. The two models are presented and related to two important phenomena: the existence, always during the discharge, of a reaction zone going from the surface to the bulk of the plate active material and the possibility, for low H_2SO_4 concentrations and high rates of discharge, of H_2SO_4 depletion, producing the reduction of the used active material. The influence of the rate of discharge and sulfuric acid concentration on potential *versus* charge curves during the discharge, on capacity and on plate resistance during the discharge transient, especially for very low discharge rate conditions are analyzed. Two equivalent plates from two different manufacturing technologies are tested. Both models, sometimes with the introduction of some modifications from traditional formulations, explain the different results found.
© 2003 Elsevier Science B.V. All rights reserved.

Keywords: Solid-state reaction model; Zone reaction mechanism; Positive plate discharge mechanism

1. Introduction

Most of the studies on the positive active material of lead–acid batteries have been on pasted positive plates [1–4]. A few papers propose and discuss models for the discharge process [5]. Studies of this mechanism on flat electrodes [6] have proposed models but they have not been compared to discharge processes in real plates [7]. As a consequence, studies on discharge mechanisms of pasted positive plates are still necessary. In the present paper, a general view of the discharge mechanism is presented based on potential/time curves, capacities, and plate resistance for different discharge rates and sulfuric acid concentrations. Two alternative models, one based on a solid-state reaction with three successive steps [8] and the other taking into account a traditional dissolution–precipitation mechanism [9] are invoked.

2. Discharge reaction models

Due to the fact that positve lead–acid battery electrodes are porous structures made of electronically conducting materials (PbO_2), the current lines will tend to go initially to the surface regions near the surface of the plate. When the discharge reaction becomes inhibited at these places, it will shift to the inner pore surfaces and this will be repeated successively until the ends of the pores are reached. The whole process needs to be seen as a zone reaction mechanism. Therefore, different discharge reaction models must be seen as happening at the reaction zone, when it is moving from the surface of the plate to its interior. The model must incorporate mechanisms that compel the reaction zone to move into the plate bulk. In other words, the models must incorporate some inhibition mechanism. As several papers do not consider the existence of a reaction zone, the corresponding proposed models do not take into account mechanisms that compel the reaction zone to move.

In the present work, two models will be presented which actually try to describe the discharge reaction mechanism at the reaction zone and these models will be used in the analysis of the present results to test their explanatory power.

One of them is the dissolution–precipitation model, based on the idea that during discharge, PbO_2 is reduced on its surface to Pb^{2+}, which goes in to solution [9]. In the solution Pb^{2+} increases in concentration, arriving at a super-saturation state and giving rise to the precipitation of $PbSO_4$ crystals. The main arguments supporting this mechanism are: the detection of $PbSO_4$ at the end of the discharge

* Corresponding author. Tel.: +55-21-16-260-8208;
fax: +55-16-260-8350.
E-mail address: dalkaine@dq.ufscar.br (C.V. D'Alkaine).

process and the fact that, on flat electrodes, the increase of the H_2SO_4 concentration over 1.0 M at constant discharge current density, i_g, and the increase of i_g at constant H_2SO_4 concentration both reduce the size of the $PbSO_4$ crystals [6]. This is because the solubility of Pb^{2+} decreases with the increase of the H_2SO_4 concentration for concentrations higher than 1.0 M [7] but also suggests that it decreases with the increase of i_g. In this model, no inhibiting mechanism that compels the reaction zone to move from the surface to the bulk of the active material has been proposed. Nevertheless, this inhibiting mechanism must be based on $PbSO_4$ crystals that will cover the whole PbO_2 surface in the reaction zone, compelling the current to move to inner surface regions of the pores. A problem with this explanation is that the observed micrographs of the $PbSO_4$ show voids between the crystals [6].

A second model [8], a solid-state reaction model, considers that the discharge reaction, happening in the reaction zone, passes through a PbO passivating film formation first step on the PbO_2 surface, through a solid-state reaction mechanism under high fields. The formation of this intermediate was demonstrated experimentally [5]. This PbO film is formed due to the high surface fields and makes the excess of O^{2-} in PbO_2 to move into the solution. The field inside the film, due to the fact that the potential is cathodic against the reversible potential, makes impossible the entry of any negative charge inside the film from the solution side, particularly the SO_4^{2-} ion that can form $PbSO_4$. The PbO_2/PbO transformation involves a current flow because it is the reduction of Pb^{4+}, in the PbO_2 matrix, to Pb^{2+} in a PbO matrix. With the increase of the thickness of the PbO inhibiting layer, the current tends to go to inner pore surface regions. Under this situation, in the originally formed PbO, the field decreases up to the moment in which a second step is possible. This is the reaction between the PbO film, without field, and the H_2SO_4. This reaction, due to the higher partial molar volume of the $PbSO_4$ than that of the PbO, gives rise to a thin passivating PbO film on PbO_2 and a disrupted $PbSO_4$ film. The small disrupted particles of $PbSO_4$, in a third stage, suffer recrystallization and give the $PbSO_4$ crystals finally observed on the surface of the active material. The discharge of the PbO_2 under the $PbSO_4$ crystals does not continue because there is always a remaining field at the $PbO_2/solution$ interface, stabilizing a thin continuous layer of passivating PbO. As a consequence, in each plate region through which the reaction zone passes, the reaction happens on the surface of the pores in three successive steps: a solid-state reduction from PbO_2 to PbO with current flow; a reaction between PbO and the H_2SO_4 to give a continuous passivating PbO thin film and disrupted $PbSO_4$ microcrystals and finally, the recrystallization of the disrupted microcrystals.

For both mechanisms, due to the fact that the formation of $PbSO_4$ consumes H_2SO_4, then, if the discharge rate is sufficiently high or the H_2SO_4 concentration sufficiently low, a depletion of H_2SO_4 in the pores can occur leading to,

the case in which there is the impossibility of the current to flow to the inner pore surfaces regions. This phenomenon reduces the depth of the discharge reaction, measured from the plate surface, in a well-known behavior giving rise to one of the mechanisms for the reduction of capacity.

3. Experiment

Galvanostatic discharges were performed on industrial stationary pasted positive plates from two different manufacturers, plates M and R. The plates were obtained from 12-V batteries with nominal $C/20$ capacities of 150 and 130 Ah/kg, for manufacturer M and R, respectively; having four positive plates per vessel for manufacturer M and five for R. The geometrical plate areas (both sides) were 280 cm^2 with a grid thickness of 0.7 mm for both manufacturers. The grid design was radial for plate R and square for plate M. The average amount of total positive charged active material for plates M was 75 g/plate and 70 g/plate for plates R. By measuring the weight of dry and wet charged active mass the average macroporosity for the two studied systems was determined. The active material of the plates M gives a porosity of $47 \pm 2\%$ and $51 \pm 2\%$ for plates R.

The alloy composition of the grids was 1.8 ± 0.2 wt.% Sb, < 0.01 wt.% Ca, <0.01 wt.% Al and 0.003 wt.% Ag for plate M and 2.6 ± 0.2 wt.% Sb, <0.01 wt.% Ca, <0.01 wt.% Al and 0.003 wt.% Ag for plate R. These data correspond to two low antimony alloys with Ag.

Both plates, before they were disassembled from the batteries, were submitted to five deep ($C/20$) discharges, inside the original battery boxes, up to a cut-off voltage (1.75 V per vessel). Between each discharge, the batteries were always recharged first at constant 4.5 A up to the battery rest voltage of 14.4 V, followed by a floating period, at this voltage, up to the moment in which the current was reduced to a value of 0.1 A per battery. At this point a new discharge was ready to start. These five cycles of charge/discharge were done to achieve stabilization of the plates.

The pasted positive plates disassembled from the batteries we re assembled stiffly, with about 1 cm separation between two negative plates, in order to keep a constant H_2SO_4 concentration in the solution during the discharge experiments. Before the discharge and after the disassembly and set-up of the experimental system, the plates were maintained charged by floating under 2.3–2.7 V, depending on the H_2SO_4 concentration. Before each discharge, the instantaneous voltages of the cells were always measured to prove that these values were higher than the corresponding reversible values, showing that the systems were overcharged.

During the discharging experiments no bending of the studied plates was ever observed, nor any shedding of the active material. The sulfuric acid concentration varied between 2.3 and 7.0 M. The discharge current was varied between 1.1 and 0.1 A. These discharge currents correspond to capacities from $C/10$ to $C/80$.

Only one plate was used for each H_2SO_4 concentration. The successive discharges of one plate (at one concentration) were made from higher to lower currents. Some of the measurements were repeated with other plates to be sure about reproducibility. This reproducibility was of the order of 5%. For the recharge, after each discharge, a constant recharge current of 0.4 A was always used first up to the moment in which $1.5\times$ the former charge of discharge had passed, followed by a floating stabilization at 2.3–2.7 V, depending on the H_2SO_4 concentration during at least 30 h.

The reference electrode was always a $Hg/Hg_2SO_4/H_2SO_4$ (4.6 M) for all H_2SO_4 concentrations used. All potentials are referred to this electrode.

4. Results and discussions

4.1. Potential/time or charge curves

Typical galvanostatic discharge plots for the two kinds of pasted positive plates, for the highest studied concentration (7.0 M H_2SO_4), are shown in Fig. 1, for different i_g. Both plates seem to be equivalent. The differences correspond to the differences between the amount of active material and porosity for the two plates.

As for tubular plates [8] all the transients present the "coup de fouet" which is reduced with the reduction of i_g and it disappears if the plate is not totally charged. The "coup de fouet" process includes a fast reduction of the potential followed by a slower increase until it reaches the potential plateau that will slowly decrease over the whole discharge. This gives rise, at the initial moments of the discharge, to a cathodic potential peak, which takes about ten minutes to evolve. If this process was the result of nucleation and coalescence of the nuclei, the potential would show an initial cathodic instantaneous fall followed by an anodic peak, so a further phenomenon must be present. One possibility must be the charging of the interface to arrive at

potentials at which the reduction reaction becomes possible. All this shows that the "coup de fouet" must be further studied even though important results have been published recently [10,11].

In Figs. 2 and 3, there are typical discharge plots for the two kinds of pasted positive plates for different acid concentrations, at a very low (Fig. 2) and a high (Fig. 3) i_g's. The decrease of the capacity C (of about 30–35%) for very low rates of discharge (Fig. 2) is in disagreement with the idea of the solid-state reaction model. For this model the final thickness of the reacted film is fundamentally determined by the final thickness of the PbO layer that, in principle, does not depend on the H_2SO_4 concentration. This dependence goes against what has been found for tubular plates under equivalent discharge conditions [8], where there was not any dependence. Nevertheless, this is in agreement with data previously found for other pasted positive plates [12]. On the other hand, the decrease cannot be related with the depletion of H_2SO_4 because, as can be seen in Fig. 2, the increase of the H_2SO_4 concentration reduces the amount of the discharge capacity obtained.

Even when this problem returns in Section 4.2, one way to explain this result from the solid-state model point of view is that in the case of pasted plates there would be some influence of the acidity at the end of the reaction of PbO_2 to PbO. It must be considered at the end because the capacity shows the total amount of the discharge when it has finished at each region of the active material pore surface, during the displacement of the reaction zone. Then, this reaction for pasted plates, can be described, at its end, by:

$$PbO_2(s) + 2H^+(sol) \Rightarrow PbO \cdot H_2O(s) \qquad (1)$$

where the H^+ enters the PbO_2 and aids to its transformation to PbO with some H_2O content. It is possible to consider that the increase of H^+ concentration in the solution reduces the thickness of the final PbO layer formed if, as is known in corrosion science, the higher the hydration of a film is, the higher is its amorphicity and the higher its passivating
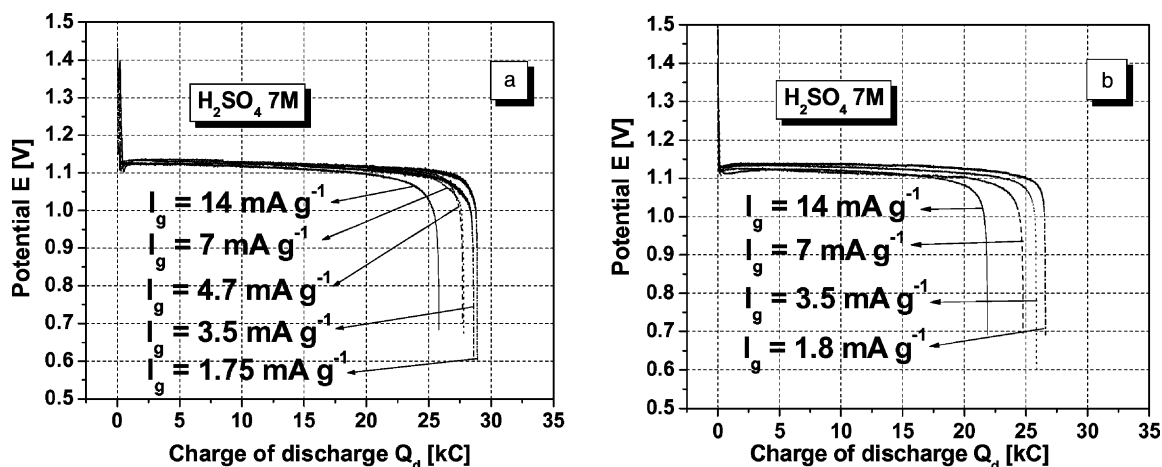
Fig. 1. Typical discharge plots for positive pasted plates at different discharge current densities shown in the figures and 7.0 M H_2SO_4 at 25 °C. (a) Plates M and (b) R. Discharge current densities in mA/g of active mass.
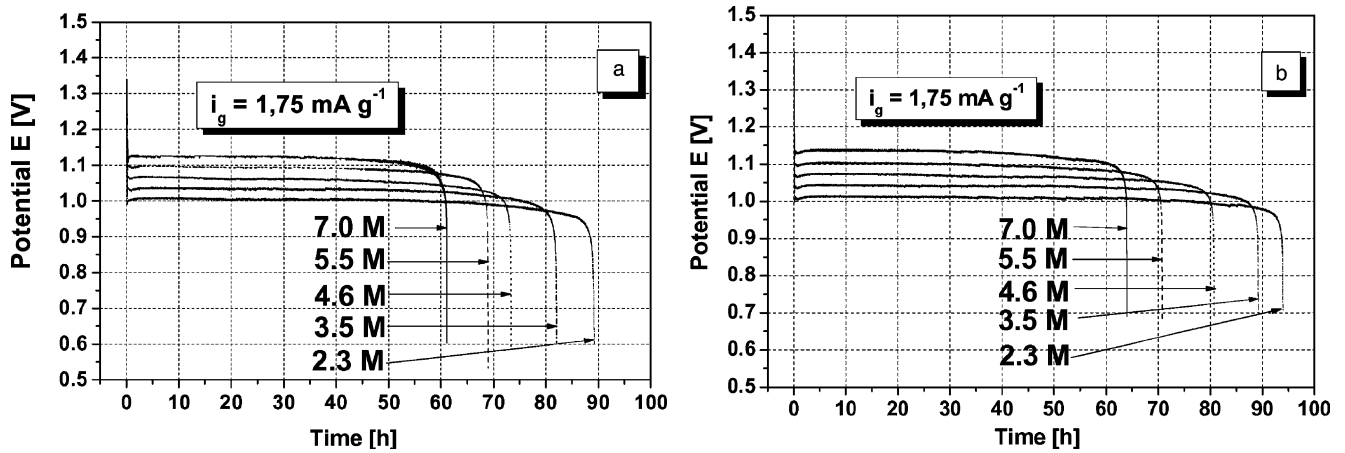
Fig. 2. Typical discharge plots at very low rate and different H_2SO_4 concentrations for the two kinds of pasted positive plates at 25 °C. (a) Plates M and (b) R. Discharge current density of 1.75 mA/g of active material for both plates.

characteristics, consequently, the lower the amount of film needed for passivation (lower the capacity). Nevertheless, the case of tubular plates [8] must be remembered where this phenomenon has not been observed. Perhaps the explanation is related to the fact that the PbO_2 coming directly from lead oxides in tubular plates (not coming from basic lead sulfates as in pasted plates) produces different kinds of structures (for example αPbO_2) in the region, which becomes transformed at the end of the PbO_2 to PbO reaction.

From the point of view of the dissolution–precipitation mechanism, in which the solubility and the supersaturation of Pb^{2+} decrease with the increase of H_2SO_4 concentration (over 1.0 M H_2SO_4), the $PbSO_4$ formation would be more and more inhibited by the increase of the H_2SO_4 concentration, giving rise to a reduction of the amount of discharging material in a way which is not totally elucidated. Nevertheless, the problem here is why this effect does not appear in the case of tubular plates.

In Fig. 3 (high i_g) can be seen the same dependence on the H_2SO_4 concentration. For these high rates of discharge, this dependence cannot be explained by H_2SO_4 depletion and as a consequence, by the reduction in the depth of the discharge region. It is the increase of H_2SO_4 concentration that reduces the capacity. This goes against considerations of H_2SO_4 depletion. This can be explained by the arguments used before, to explain the results of Fig. 2 for the two models, even when the problem for the tubular plates remains, for the dissolution–precipitation model.

All these results can be seen better through the representation of capacity C, as a function of i_g in different H_2SO_4 concentrations or in another way, by plotting C as a function of H_2SO_4 concentration at constant i_g. These kind of representations will be discussed in Section 4.2.

A last important point in relation to Figs. 2 and 3 is that with the increase of H_2SO_4 concentration there is a corresponding increase of the plateau potential for any of the
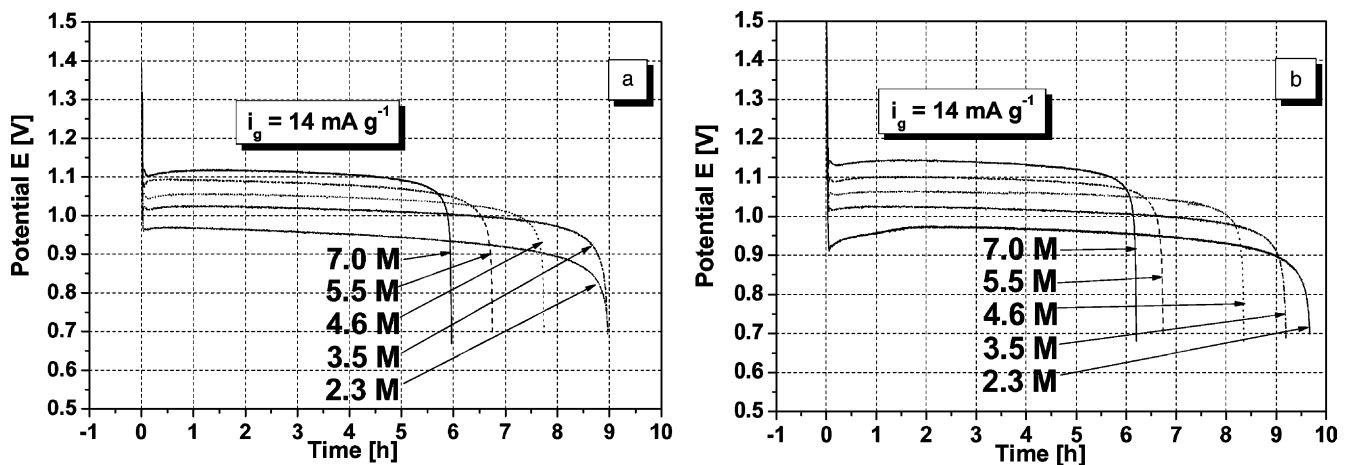
Fig. 3. Typical discharge plots at a high rate in different H_2SO_4 concentrations for the two kinds of pasted positive plates at 25 °C. (a) Plates M and (b) R. Discharge current density of 14 mA/g of active material for both plates.

analyzed discharge rates. This behavior will be discussed in Section 4.3.

4.2. The results seen at the end of the discharge processes

In Fig. 4 are plotted the results for the variation of C with i_g showing what seems to be two different types of behavior. For plate M the curves have a curvature toward the i_g axis, corresponding to the results for high i_g in a previous paper for pasted plates [12]. Nevertheless, for plates R the curvature is reversed, as happens for low i_g in the previously referred paper. Thus, case of plates R the curvature permits us to extrapolate to a maximum of C which is not dependent on the H_2SO_4, for i_g zero (C_0). This gives a result of about 170 mAg^{-1}. This is the same behavior as that obtained for pasted plates in the previous paper and recently for tubular plates [8]. The C_0 has been related to the energetic coefficient [12], the maximum amount of experimentally obtainable capacity divided by the theoretical one.

The problem seems to be with plate M, where the curves extrapolated for discharge current densities (zero) do not converge at one C_0. Instead of that, for these plates, it seems that the C_0 value depends on the H_2SO_4 concentration. For the solid-state model these results can be explained if, in plates M the curvature changes (the inflexion point) in the C/i_g plots at an i_g lower than 2.0 mAg^{-1}. On the other hand, the inflection point in the curves of plates R would be at i_g higher than 14 mAg^{-1}. If this is the correct interpretation of the data, the previous extrapolated C_0 values of plates M are not valid. They do not take into account that at lower i_g the curvature against the i_g axis will appear.

Finally, still in relation to the solid-state model, the decrease of C with increasing i_g in Fig. 4 is related to the decrease of the thickness of the PbO layer with the increase of the number of nuclei of PbO with the increase of i_g [5], with the general passivity phenomenon about the reduction of the thickness for the aging of passivating films with the increase of the growing velocity [8], due to the increase of the injection and the recombination of point defects and with the reduction of the inner plate surface with the appearance of the H_2SO_4 depletion (this last fact happening when high i_g and low H_2SO_4 concentrations are used [8]).

From the point of view of the dissolution–precipitation model, the influence of the increase of i_g on C has not been specifically analyzed in the literature. Nevertheless, the increase of i_g must be interpreted in the sense that it produces a reduction of the amount of PbSO$_4$ crystal formed and, consequently, a reduction of the capacity. This must be, perhaps, due to the influence of i_g on the necessary unstable supersaturation values for the precipitation of PbSO$_4$. This model does not present problems in relation with the influence of H_2SO_4 concentration on the extrapolated C_0 for plates M, but has no explanation for the unique C_0 value of plates R and for tubular plates [8].

In Fig. 5 the same results of Fig. 4 are seen now from another point of view. Here it is possible to see more clearly the influence of the H_2SO_4 concentrations on C. For both analyzed pasted positive plates, C increases practically linearly with the decrease of the H_2SO_4 concentration. Both results are in total disagreement with those obtained for tubular plates [8]. This is, perhaps, the most important difference found between both kinds of tubular and pasted plates and is deeply related to the results of Figs. 2 and 3.

In conclusion, from the solid-state model point of view, the dependence on the H_2SO_4 concentration in pasted plates can be related, as advanced previously, to the analyzed effect of the H$^+$ at the end of the PbO$_2$ to PbO transformation. The
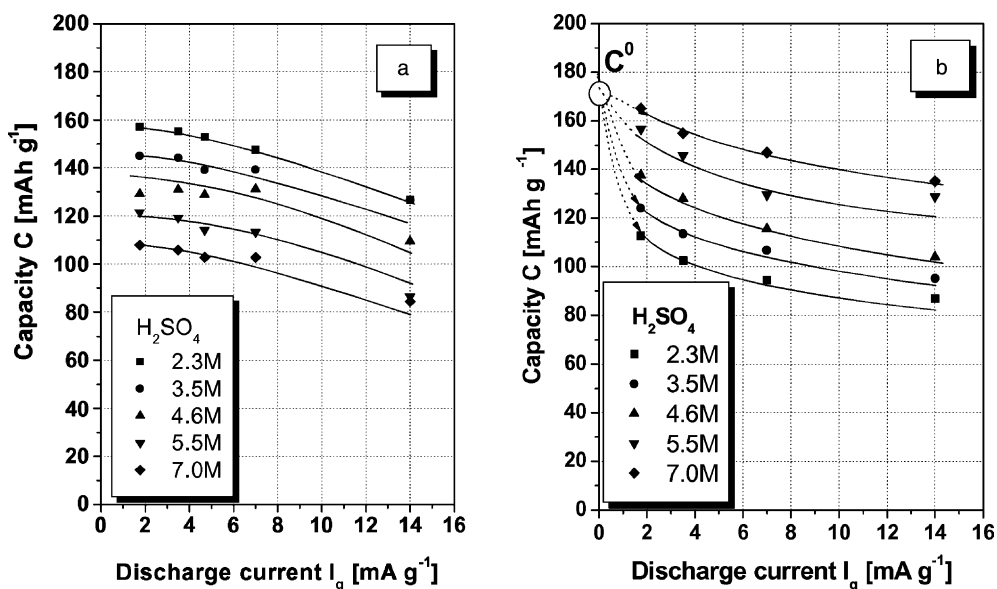
Fig. 4. Capacity (in mAh/g of active material) vs. discharge current density (in mA/g of active material), at 25 °C, for different H_2SO_4 concentrations shown in the figure. (a) Plates M and (b) R.
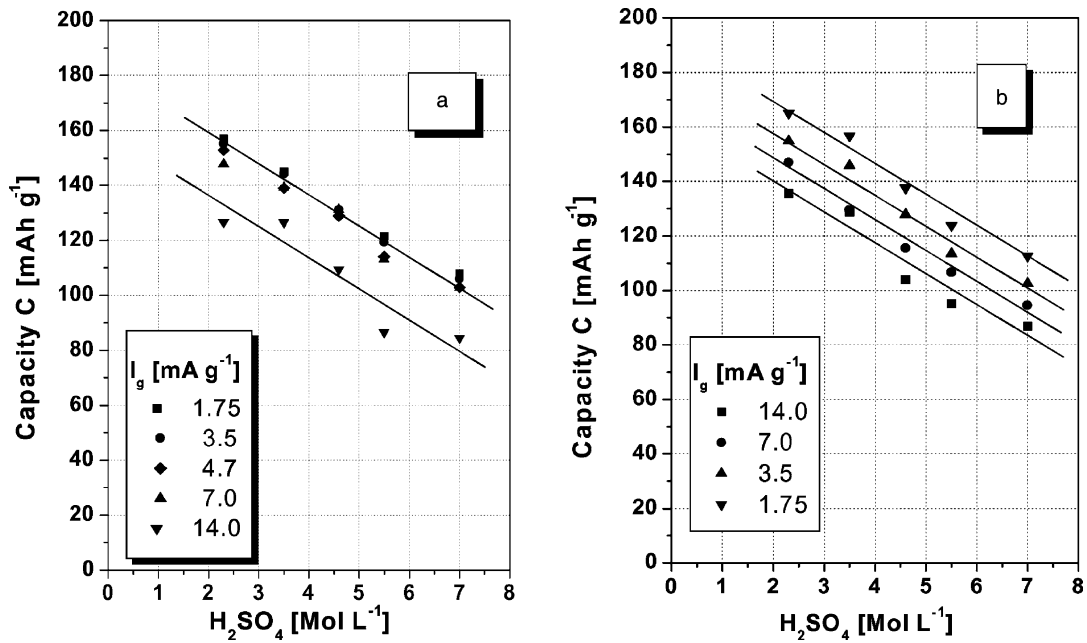
Fig. 5. Capacity (in mAh/g of active material) vs. sulfuric acid concentration at 25 °C for different discharge current densities (in mA/g of active material) shown in the figure. (a) Plates M and (b) R.

participation of the H^+ in this reaction would reduce the amount of PbO film formed due to the increase in water content, increasing the amorphicity and then, increasing the PbO passivity.

From the point of view of the dissolution–precipitation model, in relation to the H_2SO_4 concentration influence, the results seem to be more compatible due to the reduction of the Pb^{2+} solubility with the increase of H_2SO_4 concentration, but do present problems when it is necessary to explain the unique C_0 value in the cases in which it is found.

4.3. The results seen during the discharge transient on the plateau

To complete the analysis, it is important to try to understand if the ideas of the two models are in agreement with the results in the plateau regions during the transient process. In a previous paper [13], this was done for negative plates, for the solid-state model, through the determination of the resistance of the plate (r_p) at a given charge of discharge (i.e. the amount of charge, in Coulombs, withdrawn from the plate during a discharge). The resistance of a plate can be, in this case, unambiguously defined by:

$$R_p = \left(\frac{\partial E}{\partial i_g}\right)_{Q_d} \tag{2}$$

Where E is the electrode potential of the plate and Q_d is a given charge of discharge at the plateau region of the discharge. If the i_g is given in mAg^{-1}, then r_p can be obtained in ohm g.

For any model, considering the discharge as a zone reaction process, the representation of E versus i_g must give some information about the steps controlling the reaction mechanisms in a given region of the plate (at a given charge of discharge: Q_d) during the stage of the reaction that depends on the current flow. Some typical data can be seen in Fig. 6 for both kinds of plates studied. The representations give practically linear behaviors giving rise for both plates to an r_p of 1.3 ± 0.7 ohm g.

For the solid-state reaction model, the E/i_g plot will give fundamentally an average resistance of the PbO film during its growth, due to the fact that it is at the stage when there is a current flow. A straight line means that, in principle, the E/i_g in the plateau region for a given Q_d (that means at the same region of the plate) corresponds to an ohmic behavior. The resistance can be interpreted in the present case as the ionic resistivity of the film multiplied by its grams per unit of thickness. It is known in passivity that at low growth rates, that mean at low current densities, for example in a voltammetric growth, there is a linear ohmic relation between i and E [14,15]. This is why during the transient there is the E/i_g linearity.

An interesting point is that this r_p, which does not depend on i_g, also does not depend on the H_2SO_4 concentration. This last fact points suggests that the PbO_2 to PbO reaction happens in this transient region without any participation of the H^+. This result differs from that at the end of the discharge where the result depends on the H_2SO_4 concentration (see Section 4.2). This is showing that one thing is the reaction during the transient growth of the PbO and another, the end of the growth process of PbO, in a given region of the plate. The first one does not depend on the H^+ concentration while the last one does. This means that Eq. (1), giving rise to hydrated PbO, produces the passivation of the PbO_2
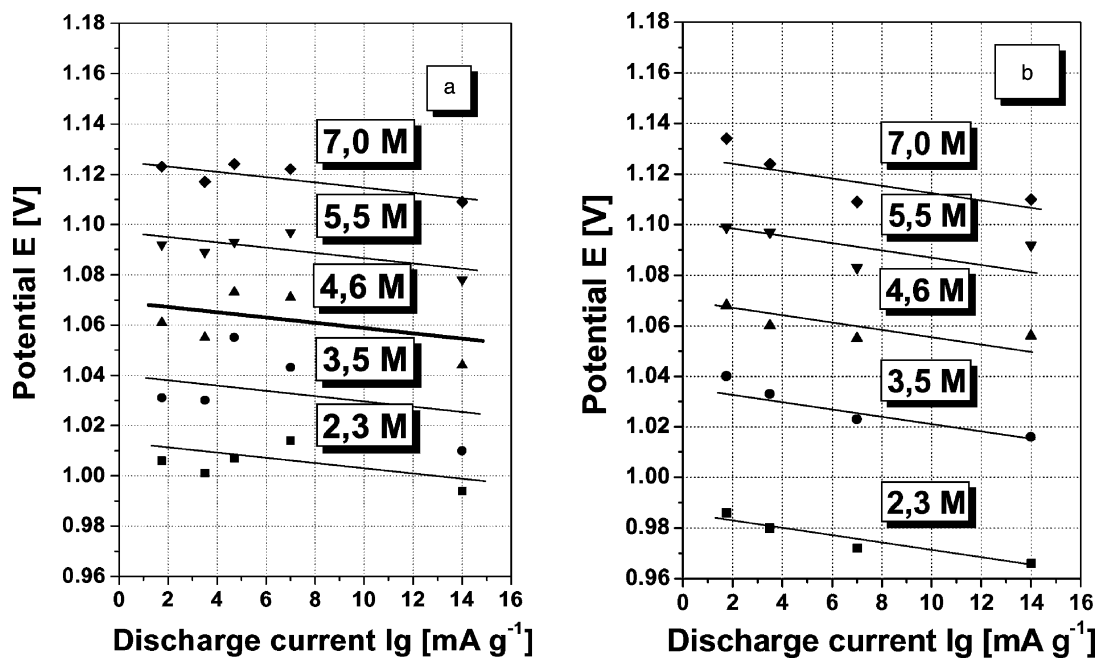
Fig. 6. Potential of the pasted positive plates versus discharge current density (in mA/g of active material) for a discharge level of 15.0 (10^3 Coulombs) in the plateau region and for different H_2SO_4 concentrations shown in the figures. (a) Plates M and (b) R.

surface so that the PbO formation comes to an end at this place.

For the dissolution–precipitation model, r_p is fundamentally determined by the transient reduction reaction of the Pb^{4+} in the matrix of the PbO_2 to the Pb^{2+} in the solution, in front of the PbO_2 surface. The linearity means in this case that this reaction would be at its linear Tafel region. This means that, in general, for this model in normal discharges, the i_g's used correspond to the linear region of Tafel plots of

this reaction. Once again there is the independence in this transient region of r_p with the H_2SO_4 concentration. In this case the results point to the fact that the transformation of Pb^{4+} (on the surface of the PbO_2) to Pb^{2+} in the solution, does not depend on the H_2SO_4 during the transient but does depend on it when the reaction comes to its end (Section 4.2).

Finally, it is important to point out that (as it has been previously stated for negative plates [13] and for positive
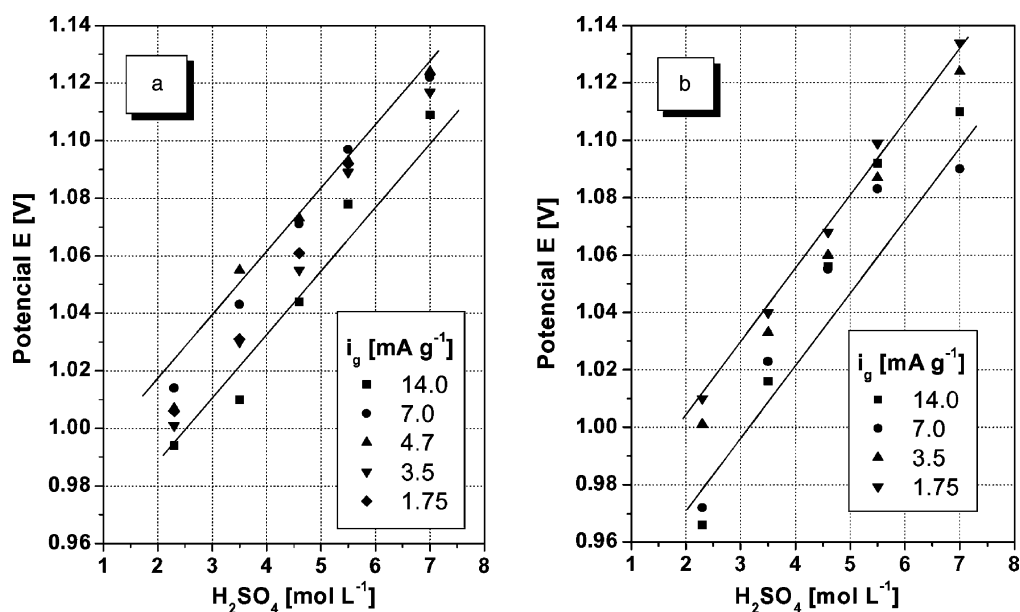
Fig. 7. Potential of the pasted positive plates versus H_2SO_4 concentration for a discharge level of 15.0 in the plateau region and for different discharge current densities shown in the figures. (a) Plates M and (b) R.

tubular plates [8]) for the present cases of pasted positive plates the representation of the same data of Fig. 6 in a plot E versus H_2SO_4 concentration, at constant i_g, also gives straight lines with always the same slope, in this case with constant positive slope. In the negative case, it gives, negative constant slopes [13]. The results can be seen in Fig. 7.

From the point of view of the solid-state model this is due to the fact that at constant Q_d and i_g, at different concentrations, the same inner surface zone of the plate is always seen at a constant overpotential, due to the constancy in r_p. Consequently, as the reversible potential changes linearly with the H_2SO_4 concentration [7], the analyzed potential must also change linearly.

For the case of the dissolution–precipitation model, the situation will be the same but now for a constant overpotential for the linear Tafel region of the passage of Pb^{4+} in the surface of the PbO_2 to Pb^{2+} in the solution.

5. Conclusions

Results for two kinds of pasted positive plates monitoring potential/time or potential/charge curves, capacity and plate resistance on the discharge plateau for discharge rates going from $C/10$ to $C/80$ with variation of the H_2SO_4 concentrations between 2.3 and 7.0 M were obtained. The behaviors found could be explained by two models reviewed in the text: a solid-state model and a dissolution–precipitation one. In both models (a) the problem that the discharge processes must follow a reaction zone mechanism going from the surface to the bulk of the plate and (b) the problem of the possible depletion of the H_2SO_4 for low H_2SO_4 concentrations and high rates of discharge, producing a reduction of the used amount of active material were considered.

For the case of the so called solid-state reaction model, passing through: (a) the formation of PbO under high field, (b) the reaction of the PbO with H_2SO_4 in the absence of the field, to give a continuous thin passivating film of PbO on the PbO_2 and a disrupted amount of $PbSO_4$ microcrystals and (c) the last step of recrystallization of these microcrystals, the results seem to be able to be interpreted through the model. Nevertheless, the H_2SO_4 concentration influence on the capacity introduces the idea that at the end of the $PbO_2/$ PbO transformation there is an H^+ effect. It is then proposed that at the end of the first step of PbO formation, the PbO becomes affected by the income of the H^+ giving a hydrated PbO, consequently, with higher amorphicity and then, higher passivity, for lower thickness, giving rise to a lower capacity.

For the case of the dissolution–precipitation mechanism, in which the reaction is the reduction of the Pb^{4+} in the matrix of PbO_2 to Pb^{2+} in the solution, followed by the increase of the Pb^{2+} concentration in the solution and finally, the precipitation of $PbSO_4$ crystals, the results also seem to be compatible with this model. Nevertheless, there is some doubt about which is the real mechanism, which makes the reaction zone move in the direction of the bulk of the plate, and here there are also some problems for the understanding of the reduction of the capacity with the increase of the discharge current.

Finally, it is shown that in the future it will be necessary to do studies about the so called ''coup de fouet'' because the present interpretations do not take into account that there is an important contribution of the charging current in this initial discharge region. Consideration of only the nucleation phenomena, with its reaction area variation, cannot explain the results found.

References

[1] S.C. Kim, W.H. Hong, J. Power Sources 77 (1999) 74–82.
[2] D.M. Bernardi, J. Electrochem. Soc. 137 (1990) 1670–1681.
[3] D. Pavlov, I. Balkanov, J. Electrochem. Soc. 134 (1987) 2390–2398.
[4] B. Culpin, J. Electrochem. Soc. 134 (1987) 2388–2390.
[5] C.V. D'Alkaine, A. Carubelli, M.C. Lopes, J. Power Sources 64 (1997) 111–115.
[6] Z. Takehara, J. Power Sources 85 (2000) 29–37.
[7] H. Bode, Lead Acid Batteries, Wiley, New York, 1977.
[8] C.V. D'Alkaine, P.R. Impinnisi, A. Carubelli, J. Power Sources, in press.
[9] E. Meissner, J. Power Sources 78 (1999) 99–114.
[10] D.W.H. Lambert, J.E. Manders, R.F. Nelson, K. Peters, D.A.J. Rand, M. Stevenson, J. Power Sources 88 (2000) 130–147.
[11] S. Piller, M. Perrin, A. Jossen, J. Power Sources 96 (2001) 113–120.
[12] C.V. D'Alkaine, A. Carubelli, H.W. Fava, A.C. Sanheza, J. Power Sources 53 (1995) 289–292.
[13] C.V. D'Alkaine, A. Carubelli, M.C. Lopes, J. Appl. Electrochem. 30 (2000) 585–590.
[14] D.E. Williams, G.A. Wright, Electrochimica. Acta 21 (1976) 1009–1019.
[15] L. Young, Anodic Oxide Films, Academic Press, New York, 1971.